Available online at www.sciencedirect.com
SCIENCE DIRECT®
Polymer 45 (2004) 385–398
polymer
www.elsevier.com/locate/polymer

Synthesis and nitrosation of processible copolymers from pyrrole and ethylaniline

Xin-Gui Li[a,b,c,*], Mei-Rong Huang[a], Mei-Fang Zhu[b], Yan-Mo Chen[b]

[a]*State Key Laboratory of Concrete Materials Research, Institute of Materials Chemistry, College of Materials Science and Engineering, Tongji University, 1239 Siping Road, Shanghai 200092, China*
[b]*State Key Laboratory for Modification of Chemical Fibers and Polymer Materials, Donghua University, Shanghai 200051, China*
[c]*Shanghai Key Laboratory of Molecular Catalysis and Innovative Materials, Fudan University, Shanghai 200433, China*

Received 24 July 2003; received in revised form 25 October 2003; accepted 12 November 2003

Abstract

A series of copolymers were prepared by an oxidative polymerization of pyrrole (PY) and 2-ethylaniline (EA) in HCl. The polymerization process was followed by tracking open-circuit potential and temperature of the reaction solutions. The fine particles of the PY/EA copolymers obtained in situ were further *N*-nitrosated for the first time in order to improve their solubility. The size, structure, and properties of the fine particles and their *N*-nitroso products were systematically characterized by laser particle size analyzer, FTIR, UV–vis, GPC, solution casting, and TG techniques. It is found that both the open-circuit potential and temperature of the solutions exhibit a maximum during the copolymerization, while the particle size of the copolymers will decrease monotonically with prolongating polymerization time or doping. Both the polymerization yield and molecular weight of the copolymers exhibit a minimum with PY/EA ratio, indicating a mutual retarding effect between the PY and EA monomers. The top potential and top temperature of the copolymerization as well as the particle size and its distribution, solubility, film-forming ability, electroconductivity, and thermostability of the copolymers all depend significantly on the PY/EA ratio. The PY/EA copolymers have good solubility in the solvents with the solubility parameter from 23 to 27 $J^{1/2}/cm^{3/2}$, dielectric constant greater than 12 and polarity index from 6.4 to 7.4 and their solubility becomes further better with increasing EA content. The *N*-nitrosation of copolymers can also improve their solubility in polar solvents furthermore. The copolymers with PY content of less than 30 mol% in NMP and THF exhibit good thin-film formability. The copolymer films become smoother and tougher with increasing EA content and by *N*-nitrosation. With increasing PY content, the decomposition temperature, maximum decomposition rate, char yield at 500 °C, and activation energy all decrease but decomposition order increases. The temperature at the maximum weight-loss rate of the copolymers has a maximum at the PY/EA molar ratio of 30/70. These results suggest that the polymer obtained is a real copolymer containing two comonomer units.

Keywords: Pyrrole copolymer; *N*-nitrosation; Film formability

1. Introduction

Electroconductive polymers have attracted a great deal of attention, mainly due to their potential applications in a variety of new technologies, such as electronic devices [1], electrochromic displays [1,2], rechargeable batteries [1,3], polymer-modified electrodes [4], functional film [5], biosensors [6,7], and anticorrosion primer layers [8,9]. Conducting polymers which are the focus of considerable current research can be classified: (a) polyacetylene, (b) poly(*p*-phenylene), (c) polyaniline, and (d) polyheterocycles. The former classes (a) and (b) exhibit high electrical conductivity, which can reach to 10^{5-7} s cm^{-1} [10,11], but their poor stability restricted the wide application. Polypyrrole (PPY), polyaniline (PAN), and polythiophene in the classes (c) and (d) not only feature relatively high electroconductivity up to 10^{3} s cm^{-1} [12], but also are much more stable than polyacetylene and poly(*p*-phenylene). In addition, PPY, PAN and polythiophene can be

* Corresponding author. Tel.: +86-21-65799455; fax: +86-21-65980530. Current address: Institute of Materials Chemistry, State Key Laboratory of Concrete Materials Research, College of Materials Science and Engineering, Tongui University, 1239 Siping Road, Shanghai 200092, China.
E-mail address: xinguili@163.com (X.G. Li).

0032-3861/$ - see front matter © 2003 Elsevier Ltd. All rights reserved.
doi:10.1016/j.polymer.2003.11.014

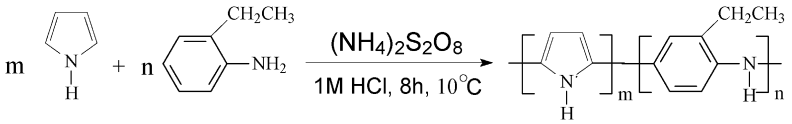

Scheme 1.

much more easily prepared by an oxidative polymerization. Considering much higher cost of thiophene than pyrrole (PY) and aniline, PPY and PAN should be the most attractable conducting materials with brilliant industrial foreground.

Only one blemish for PPY seems its poor processability. For example, PPY is both insoluble and infusible as well as its film is hard and usually brittle. In fact, the poor processability has strongly affected the formation and extensive application of PPY. Therefore, the improvement of the processability becomes very important and necessitous. In addition, π-conjugated polymers containing flexible aliphatic side groups have been one of the major subjects of recent interest. For example, poly(2-ethylaniline) (PEA) has much better solubility than PPY and PAN [13] and its film can be easily formed by a solution route, though its electrical conductivity is not good as those of PPY and PAN [14,15].

It has been widely reported that the oxidation potential of PY monomer is 1.19 [16], or 1.0, or 0.65 [17] with an average value of 0.95 V vs. SCE as well as the oxidation potential of 2-ethylaniline (EA) monomer is 0.86 V [18] vs. SCE. Therefore, the both monomers are provided with essential conditions for the formation of their oxidative copolymer. In this article, a series of copolymer particles were directly prepared by a heterohomogeneous oxidative copolymerization of PY and EA in HCl, and further *N*-nitrosated in sodium nitrite solution in HCl to significantly and furthermore improve the solution processability. The dependence of the diameter and its distribution of the copolymer particles on PY/EA ratio, polymerization time, and *N*-nitrosation is systematically investigated for the first time. The macromolecular structure and thermostability of the fine particles are elaborated. In particular, a good solubility and uncommon film formability of the PY/EA copolymers are proposed.

2. Experimental

PY, EA, $(NH_4)_2S_2O_8$, HCl, $NH_3{\cdot}H_2O$, $NaNO_2$, dimethylsulfoxide (DMSO), and *N*-methyl-pyrrolidone (NMP), *N*,*N*-dimethylformamide (DMF), formic acid, *m*-cresol, H_2SO_4, $CHCl_3$, tetrahydrofuran (THF), and toluene were commercially obtained and used as received.

2.1. Polymerization

A representative procedure of the oxidative polymerization for a direct formation of the fine particles of the PY/EA (50/50) copolymer is as follows: To 50 ml of a 1 M HCl aqueous solution, 1.808 ml (25 mmol) of PY and 3.154 ml (25 mmol) of EA were added into a 100-ml, two-necked glass flask in a water bath and magneto-stirred vigorously for 30 min. Ammonium persulfate [$(NH_4)_2S_2O_8$; 5.82 g, 25 mmol] was dissolved separately in 50 ml of 1 M HCl to prepare an oxidant solution. The monomer solution was then treated with the oxidant solution (oxidant/monomer, 1/2 mol) added dropwise at 10 °C in 30 min. After the first few drops, the reaction solution turned bottlegreen. The reaction mixture was further magneto-stirred for 8 h in the water bath at 10 °C. The copolymer HCl salt particles, called as the original doped PY/EA polymer in this article, were isolated from the reaction mixture by filtration and washed with an excess of distilled water to remove the oxidant and oligomers. Half of the HCl salt was subsequently neutralized in 125 ml of 0.2 M $NH_3{\cdot}H_2O$ for 16 h for the preparation of a base form of the PY/EA copolymer particles, called as the dedoped PY/EA polymer. Then the HCl salt and base form of the copolymer particles were dried, respectively, at 40 °C for 3 days and two kinds of black powders were left. The copolymer HCl salt (0.91 g) and the copolymer base (0.93 g) were obtained with a yield of 40.7%. The nominal reaction was shown in Scheme 1.

2.2. N-Nitrosation and de-nitrosation reactions

The *N*-nitroso PY/EA copolymer was prepared via nitrosation reaction described previously [11]. To 50 ml of a 2 M HCl solution, 1 g of copolymer particles was added to a 100 ml glass flask and magneto-stirred vigorously for several hours. Then sodium nitrite (50 ml of 0.15 M $NaNO_2$) was also slowly added to the glass flask at 0 °C. The reaction mixture was stirred at 0 °C for 24 h, and then water was added to terminate the reaction. The *N*-nitroso copolymer HCl salt, called as the *N*-nitroso doped polymer

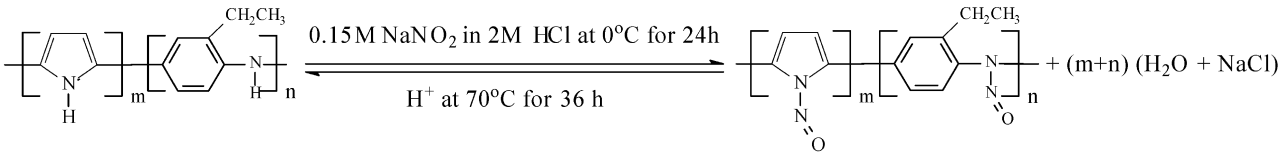

Scheme 2.

Table 1
Chemically oxidative polymerizations with nine pyrrole/2-ethylaniline ratios at the oxidant/monomer molar ratio of 1/2 in 1 M HCl for polymerization time of 8 h

PY/EA molar ratio	Initial/top temperature T_1/T_2(°C)	$\Delta T(T_2 - T_1)$(°C)	Time of darkling of reaction solution (s)	Color of polymer particles[a]	
				Salt	Base
0/100	9.2/10.8	1.6	120	BO	MO
5/95	11.3/15.3	4.0	90	BO	SC
10/90	10.4/12.5	2.1	80	BO	Bl
20/80	15.8/19.2	3.4	30	BO	BO
30/70	9.9/13.3	3.4	15	BO	Bl
50/50	10.5/13.5	3.0	27	Bl	Bl
70/30	6.3/10.6	4.3	12	Bl	Bl
90/10	10.2/14.6	4.4	12	Bl	Bl
100/0	10/–	–	–	Bl	Bl

[a] BO, Bottlegreen; MO, Modena; SC, Scarlet; Bl, Black.

in this article, was isolated from the reaction mixture by filtration and washed with an excess of distilled water to remove residual $NaNO_2$ and by-product. One third of the HCl salt was subsequently neutralized in 50 ml of 0.2 or 0.02 M $NH_3{\cdot}H_2O$ for 36 h to obtain base form of the *N*-nitroso copolymer, called as the *N*-nitroso dedoped polymer with 0.2 or 0.02 M $NH_3{\cdot}H_2O$. The *N*-nitroso copolymers were all washed with excess water. Then the HCl salt and base forms of *N*-nitroso copolymer were dried, respectively, under vacuum for 5 days and three types of black powders were left. The whole *N*-nitrosation reaction was shown in Scheme 2.

The de-nitrosation reaction, as shown in Scheme 2, is very simple as compared with the nitrosation reaction. After the dark red *N*-nitroso polymer was heated at 70 °C for 36 h, the dark product, called as the de-nitroso polymer, was gained.

2.3. The measurements of solubility and film formability

10 mg of the copolymer powder was added to 1 ml of solvent and dispersed thoroughly After the mixture was swayed intermittently for 24 h at room temperature, the solubility of the polymers could be characterized semi-quantitatively. The four better solvents, such as NMP, DMSO, formic acid and THF, were further used for the measurement of the film formability of the copolymers by using the following method: 50 mg of the polymer powder was added to 1 ml of solvent and dispersed thoroughly. After it was swayed intermittently for 3 days at room temperature the solution was dropped onto the flat glass and dried at 70 °C for 3 days. After the solvent evaporated completely the films with the area of 3–10 cm^2 were peeled off.

2.4. Characterization

The potential of the reaction solution during the copolymerization was measured by the open-circuit potential technique, using a saturated calomel electrode (SCE) as standard electrode and a Pt electrode as working electrode. A laser scattering particle-size analyzer (Beckman Coulter LS230) was used to measure the size and its distribution of original and *N*-nitroso copolymer particles. An IR spectrophotometer (Magna-IR™ Spectrometer 550, Nicolet) was used to identify chemical structures of the polymers by mixing the particles with KBr and then pressing the mixtures into tablets. UV–vis spectra were recorded in formic acid using a UV–vis–NIR spectrophotometer (Perkin–Elmer instruments, Lambda 35) in the wavelength range 190–1100 nm. Molecular weight (MW) and its distribution were measured by using HP1100 gel permeation chromatography column (PL-gel mixed C × 2, PL gel 50 nm) as well as THF as solvent and mobile phase. Monodisperse polystyrene with MW ranging from 500 to 10^6 g/mol was used as standards. The bulk electrical conductivity of a pressed disk with the thickness of 0.1 cm for the PY/EA copolymers was measured by a two-probe method at 20 °C. A Perkin–Elmer Thermogravimetric Analyzer Pyris 1 TGA was used to measure the weight loss of the polymers with the sample size of 2.3–3.0 mg in air. The film thickness was measured by using the thickness gauge made in China.

3. Results and discussion

3.1. Temperature and potential of the copolymerization solutions

The effect of PY/EA ratio on the oxidative copolymerization at oxidant $(NH_4)_2S_2O_8$/monomer molar ratio of 1/2 in HCl is listed in Table 1 It is found that with an increase in PY content, the ascend degree (ΔT) of solution temperature during polymerization shows a basically increasing trend, and the time of darkling of reaction solution during

Table 2
Particle size of virgin doped and dedoped PY/EA (5/95 and 20/80) copolymers with oxidant [$(NH_4)_2S_2O_8$]/monomer molar ratio of 1/2 in 1 M HCl at different polymerization times

Polymerization	PY/EA molar ratio	Polymn. time (h)	Mean size (μm)	SD (μm)	CV (%)
Doped virgin salt particles	5/95	0.5	13.1	8.08	61.9
		2	10.8	5.83	54.3
		8	6.92	5.33	76.9
		12	3.79	2.71	71.6
	20/80	0.5	10.1	3.85	38.3
		2	8.28	3.34	40.3
		8	4.43	2.14	48.4
Dedoped emeraldine base particles	5/95	0.5	12.7	7.79	61.3
		1	12.8	7.86	61.5
		2	12.5	8.73	66.1
		4	11.8	8.17	69.4
		8	8.12	6.21	76.5
		12	6.16	4.92	79.8
	20/80	0.5	10.1	3.89	38.5
		1	9.70	3.82	39.3
		2	8.93	3.65	40.8
		4	7.16	3.34	46.6
		8	5.96	2.58	43.3
		12	4.83	2.32	48.1

dropping oxidant shortens, and the color of final polymer obtained changes from bottlegreen to black. These facts suggest that the copolymerization of PY and EA monomers is exothermic. Moreover PY monomer engenders more heat than EA monomer during the polymerization because of higher oxidative reactivity of PY monomer. Considering that the oxidation potentials of PY and EA monomers are 0.95 and 0.86 [18] (*V* vs. SCE) respectively, lower reactivity of EA monomer must result from lower initiation reactivity induced by a big steric hindrance of the ethyl group on the phenyl ring. Relatively low increase of reaction temperature and long darkling time during PY/EA (50/50) copolymerization could be due to relatively slow dropping rate of the oxidant solution in the earlier 20 min of polymerization,

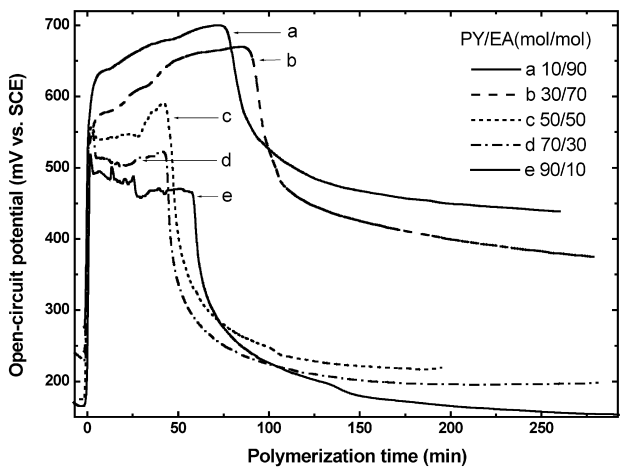

Fig. 1. The open-circuit potential of the PY/EA copolymerization solution with different molar ratios with polymerization time.

while a relatively high temperature increase and short darkling time of PY/EA (5/95) system could be due to the relatively fast rate of dropping oxidant.

The PY/EA copolymerization was followed by an open-circuit potential technique, as shown in Fig. 1. The potential of all polymerization solutions increases sharply to the first inflexion (P_1) in several minutes, which is the first step of polymerization reaction. The increase of solution potential is due to dropping oxidant with high potential. Then the potential smoothly reaches the second inflexion (P_2) in 50–100 min, depending on PY/EA ratio, corresponding to the second step of polymerization reaction. When PY content is not larger than 50 mol%, the solution potential at the second step shows a clear increasing trend. At a PY content of 70 mol%, the solution potential at the second step appears substantially constant. On the contrary, at a PY content of 90 mol%, the solution potential at the second step shows a clear decreasing trend. The absolute value of the solution potential at the second step decreases monotonically from 630–700 to 470–520 mV vs. SCE with increasing PY content from 10 to 90 mol%. The continuance time of the second step exhibits a decreasing tendency from 90 to 45 min with increasing PY content from 10 to 70 mol%. These imply that the copolymerization speeds up with increasing PY content. That is to say, the steric effect of the ethyl group on aniline ring slows down the polymerization (propagation) rate. It should be pointed out that the polymerization solution temperature has reached the maximum value when the potential profile passes P_2 and begins to decline sharply, implying that P_2 is a turning point of molecular chain propagation. Relatively longer continuance time of the second step of the PY/EA (30/70 and 90/10)

Table 3
The influence of *N*-nitrosation on the particle size of PY/EA (5/95 and 20/80) copolymers with oxidant $[(NH_4)_2S_2O_8]$/monomer molar ratio of 1/2 in 1 M HCl

PY/EA molar ratio	Copolymer particle form	*N*-Nitrosation time (h)	Mean size (μm)	SD (μm)	CV (%)
5/95	Doped virgin salt	0	12.49	9.39	75.1
		12	6.965	5.82	83.5
	Dedoped emeraldine base	0	12.44	9.30	74.7
		12	8.05	6.72	83.5
20/80	Doped virgin salt	0	5.12	2.87	55.9
		12	4.23	2.13	50.3
	Dedoped emeraldine base	0	5.22	3.02	57.7
		12	3.65	1.88	51.5

copolymerizations should be due to relatively low dropping rates of oxidant. The copolymerization turns into the third step after the open-circuit potential passes P_2. The open-circuit potential gradually inclines to a limiting minimum value (P_{min}) with the prolongation of polymerization time. P_{min} mainly represents the potential of PY/EA copolymer. The P_{min} value also steadily decreases from 440 to 150 mV vs. SCE with increasing PY content from 10 to 90 mol%, indicating that the consumption of the oxidant tends complete.

3.2. The formation and characterization of the fine particles in water

The fine particles of PY/EA copolymers have been easily and directly gained by a heterohomogeneous oxidative polymerization Similarly, the fine particles of *N*-nitroso copolymers can also be prepared expediently via *N*-nitrosation. All of the distribution curves of the particle sizes are substantially normal together with characteristics of a tail of larger particle sizes. The dependency of the particle size and its distribution on polymerization time, polymer form, and the incorporation of nitroso group, is discussed in detail below.

3.2.1. The variation of the particle sizes with polymerization time

Particle size of original doped PY/EA (5/95, 20/80) copolymers with an oxidant $[(NH_4)_2S_2O_8]$/monomer molar ratio of 1/2 in 1 M HCl at different polymerization times is described in Table 2 With prolongating polymerization time the size and its distribution (standard deviation (SD)) of the particles decrease, while the coefficient of variation (CV) of particle size distribution exhibits an increasing tendency. The phenomena should be mainly due to the comminuting effect from the mechanical force during magneto-stirring, making loose or porous particle aggregates [19] formed at the beginning of copolymerization comminute into relatively compact, nonporous, and uniform small particles at the end of reaction. The mean size of all the copolymer particles obtained is smaller than the mean size (15 μm) of homologous particle measured by Kim et al. [20]

Particle sizes of dedoped PY/EA (5/95 and 20/80) copolymers at different polymerization times are shown in Table 2. Apparently, dedoped PY/EA (5/95 and 20/80) copolymers exhibit larger particle size and wider size distribution than original doped PY/EA (5/95 and 20/80) copolymers. That is to say, a dedoping process by $NH_3{\cdot}H_2O$ makes the particles slightly larger, implying a possible swell or conglomeration of the smaller particles after the exclusion of HCl doping molecules. With prolongating polymerization time, the particle size decreases, and the SD decreases dramatically, but the CV increases substantially, resembling original doped copolymers.

3.2.2. The variation of particle size with N-nitrosation

The influence of *N*-nitrosation on the size distribution of PY/EA (5/95 and 20/80) copolymer particles is listed in Table 3. It is obvious that the particle sizes and their SD clearly shift to smaller value after *N*-nitrosation for 12 h,

Table 4
The molecular weight and polydispersity index of PY/EA copolymer bases in THF

PY/EA molar ratio	Base form	$\bar{M}_n$ (g/mol)	$\bar{M}_w$ (g/mol)	$\bar{M}_z$ (g/mol)	$\bar{M}_w/\bar{M}_n$	$\Delta(\bar{M}_w/\bar{M}_n)$ between emeraldine and *N*-nitroso bases
0/100	Emeraldine	5619	15,090	39,710	2.68	–
5/95	Emeraldine	3360	11,240	29,600	3.35	1.65
	N-Nitroso	3374	16,870	72,410	5.00	
20/80	Emeraldine	4312	17,730	55,120	4.11	1.12
	N-Nitroso	4961	25,960	131,700	5.23	
30/70	Emeraldine	7195	20,910	52,370	2.91	0.09
	N-Nitroso	7216	21,610	52,160	3.00	

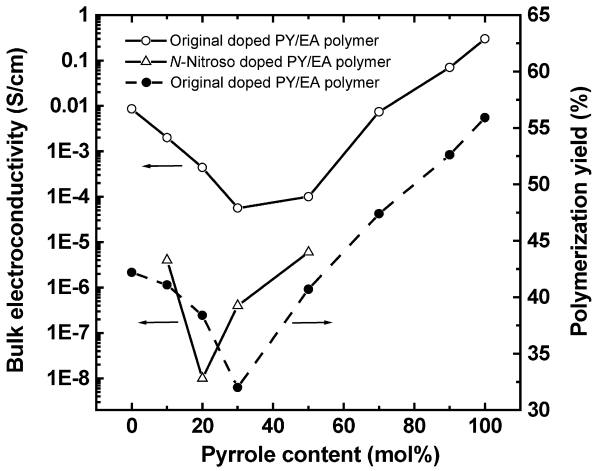

Fig. 2. The dependence of polymerization yield (●) and bulk electroconductivity of the PY/EA copolymer virgin salts (○) and their *N*-nitroso product (△) on the PY molar content.

probably due to additional mechanical force of magneto-stirring or the compaction inside the particles after *N*-nitrosation. Although the particle diameter of the doped and dedoped copolymers does not change much after *N*-nitrosation for about 1 h, the dedoped particles of PY/EA (5/95) copolymer have larger diameter and SD than doped particles after 12 h *N*-nitrosation, because the dedoped particles themselves exhibit smaller diameter and SD before *N*-nitrosation. The variation of the particle diameter seems contrary for the PY/EA (5/95) copolymer with *N*-nitrosation.

3.3. Copolymerization yield and molecular weight of PY/EA copolymers

It is interesting that with increasing PY content from 0 to 100% the polymerization yield exhibits a minimum at PY/EA molar ratio of 30/70 as shown in Fig 2, implying a clear and strong copolymerization effect. A similar minimal yield was also observed for the copolymerization of PY with *o*-phenetidine [21]. The probable reason is that copolymerization reactivity of PY with aniline derivatives is lower than their homopolymerization reactivity. That is to say, the two types of monomers appear retarder each other.

The MW and polydispersity index of the bases and *N*-nitroso derivatives of the PY/EA copolymers are listed in Table 4. It is easily discovered that as the PY content increases from 0 to 30 mol%, the copolymers exhibit a minimum MW at the PY/EA molar ratio of 5/95, apparently due to a mutually retarding copolymerization effect between PY and EA monomers. It suggests that a small amount of PY monomer can retard oxidative polymerization of EA monomer, again proving a mutual retarding action between the two monomers, which is the same as the results based on the polymerization yield. This is another evidence that the polymer formed is a real copolymer rather than a simple mixture of two homopolymers. It is seen that EA homopolymer has the lowest polydispersity index ($\bar{M}_w/\bar{M}_n$) of 2.68, whereas the PY/EA (20/80) copolymer exhibits the highest ($\bar{M}_w/\bar{M}_n$) of 4.11. It appears that polymerization (propagation) reactivity of PY monomer is higher than EA monomer. Note that the variation of the MW of the copolymers with PY/EA molar ratio from 5/95 to 30/70 is just opposite to that of the yield. That is to say, with increasing PY content from 5 to 30 mol%, the polymerization yield decreases but the MW increases. This might suggest that the chain initiation activity decreases but the chain propagation activity increases with increasing PY feed content. The MW of the copolymers with more than 30 mol% PY content is not listed in Table 4 because of their insolubility in THF, as listed in Table 5. It should be noted that this study gives much higher polymerization yield and higher MW of the EA homopolymer than earlier literature (yield, 16% and MW, 5000) [15], indicating the oxidative

Table 5
The solubility of the PY/EA copolymers obtained with $(NH_4)_2S_2O_8$/monomer/HCl molar ratio of 1/2/4 for polymerization time of 8 h

Solvent	Solubility[a] of PY/EA copolymers and solution color[b]							
	Salt/base (0/100)	Base (5/95)	Salt/base (10/90)	Salt/base (20/80)	Salt/base (30/70)	Salt/base (50/50)	Salt/base (90/10)	Salt/base (100/0)
NMP	S(B)/S(B)	PS(B)	MS(UL)/MS(U)	PS(B)/PS(B)	PS(Bl)/PS(U)	PS(Bl)/PS(Bl)	PS(Bl)/PS(Bl)	IS/IS
DMSO	PS(B)/PS(B)	MS(B)	PS(Bl)/MS(Bl)	PS(C)/PS(B)	PS(Bl)/MS(Bl)	SS(Bl)/PS(Bl)	PS(Bl)/PS(Bl)	IS/IS
DMF	SS/S(B)	PS(B)	PS(Bl)/MS(U)	PS(B)/PS(B)	PS(Bl)/PS(U)	PS(Bl)/PS(Bl)	PS(Bl)/PS(Bl)	IS/IS
Formic acid	S(BO)/S(BO)	S(BO)	S(BO)/S(BO)	PS(G)/PS(G)	PS(Bl)/MS(Bl)	PS(Bl)/PS(Bl)	SS(Bl)/PS(Bl)	IS/IS
m-Cresol	S(BO)/S(BO)	PS(LB)	MS(BO)/MS(U)	PS(G)/PS(B)	IS/IS	PS(Bl)/PS(Bl)	PS(Bl)/PS(Bl)	IS/IS
H_2SO_4	S(RM)/S(RM)	PS(M)	PS(M)/PS(M)	PS(Bl)/PS(M)	PS(M)/PS(M)	IS/IS	IS/IS	IS/IS
$CHCl_3$	IS/PS(BO)	PS(BO)	IS/S(BO)	IS/S(BO)	IS/PS(BV)	IS/IS	IS/IS	IS/IS
THF	IS/S(BO)	PS(BO)	IS/S(BO)	IS/S(BO)	IS/PS(LB)	IS/IS	IS/IS	IS/IS
CH_2Cl_2	IS/MS(BO)	PS(BV)	IS/S(BV)	IS/S(BV)	IS/PS(LV)	IS/IS	IS/IS	IS/IS

[a] S, soluble; MS, mainly soluble; PS, partially soluble; SS, slightly soluble; IS, insoluble.
[b] The letters in the parentheses mean solution color. B, blue; Bl, Black; BO, bottlegreen; BV, blue violet; C, cyan; DM, dark maroon; G, green; Gr, gray; LB, light blue; LM, light mauve; LV, light violet; M, maroon; Ma, mauve; MO, modena; RM, red–maroon; RO, red–orange; SC, scarlet; U, ultramarine; Y, yellow; YM, yellow–maroon.

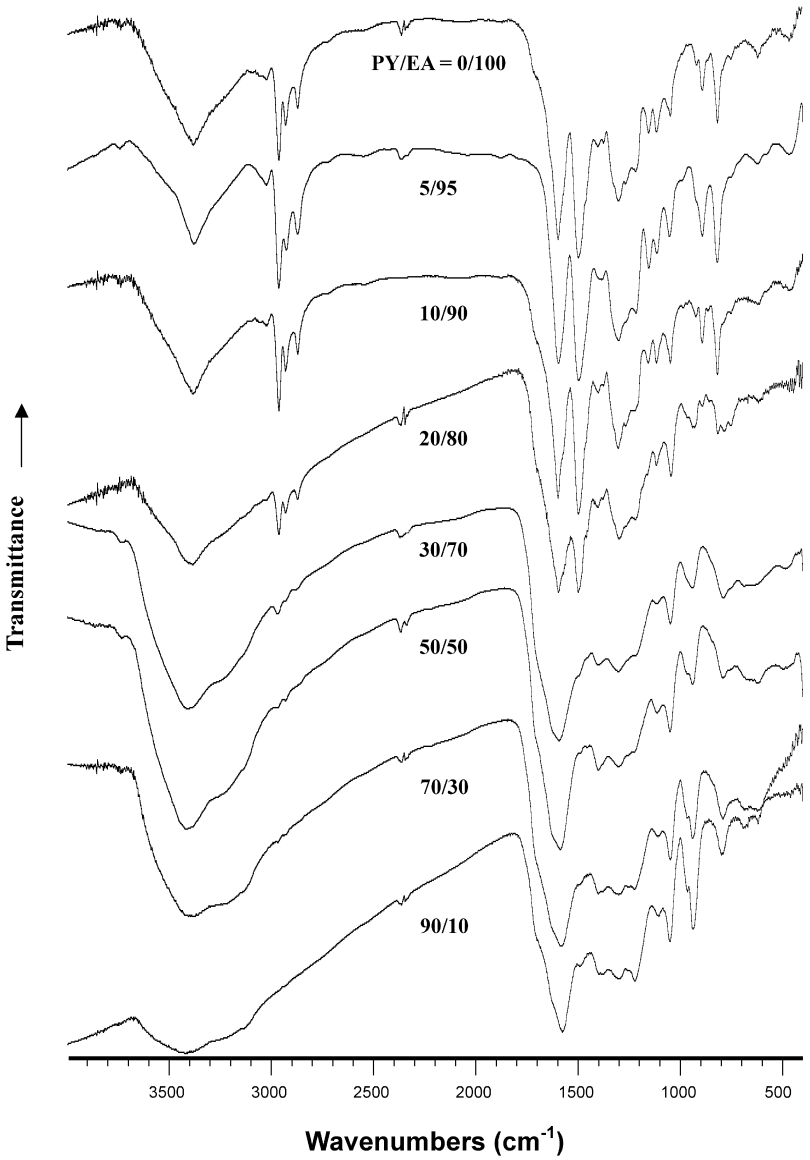

Fig. 3. IR spectra of PY/EA copolymer bases (dedoped form) with different PY/EA molar ratios.

polymerization condition designed in this study is optimal to some extent.

It can also be seen from Table 4 that the *N*-nitroso copolymers have slightly higher MW and polydispersity index than corresponding un-nitroso copolymers, due to the incorporation of polar *N*-nitroso groups [11]. The difference $\Delta(\bar{M}_w/\bar{M}_n)$ of polydispersity index between emeraldine and *N*-nitroso forms decreases with increasing PY unit content, i.e. the variation of the polydispersity index with *N*-nitrosation becomes smaller for the copolymers with more PY content.

3.4. IR spectra

IR absorption spectra of the copolymer bases (dedoped form) with eight PY/EA ratios are shown in Fig. 3. A single band centered at 3400 cm^{-1} due to the characteristic N–H stretching vibration suggests the presence of –NH– groups in PY and EA units. In contrast to two peaks of the $-NH_2$ stretching, this single peak due to the N–H stretching of secondary amine reflects that most of primary amine $-(NH_2)$ groups has participated in polymerization. The single band becomes weaker and broader and shifts to higher wave number with an increase in PY content from 0 to 90 mol%. It is accordant with the report that PPY hardly ever exhibits –NH– vibration peak [22,23]. Two weak peaks from 3000 to 2850 cm^{-1} should be due to aromatic and aliphatic C–H stretching vibrations, respectively. With increasing PY content, both of the two peaks become weaker and finally almost disappear because PY unit contains less aromatic C–H bonds and does not contain any aliphatic C–H bond. Thus the characteristics of IR spectra of the copolymers above 2000 cm^{-1} are dominated by the EA units. However, the IR absorption below

2000 cm^{-1} is also influenced by the PY units. The absorption intensity at 1498, 1300, 1110, and 820 cm^{-1} significantly gets weaker with increasing PY content, whereas the absorption intensity at 1600, 1210, 1050, and 940 cm^{-1} steadily and continually gets stronger. The enhanced absorption peaks should be attributable to PY unit to some extent because the bands at 1570, 1180, and 890 cm^{-1} are characteristic of PPY [24,25]. The variation of the intensity of these peaks might result from the copolymerization effect between PY and EA monomers. So it is concluded that the PY unit in the polymer chains exists mainly in the quinoid form. A similar phenomenon was also observed for the copolymerization of PY with *o*-anisidine [26]. These results suggest the formation of real copolymers between PY and aniline derivative monomers again.

It should be noted from Fig. 3 that a dramatic difference between the IR spectra of the PY/EA (20/80 and 30/70) copolymers in the whole wavenumber range is found, indicating that their macromolecular structures are quite different. In other word, the chain structure of the PY/EA (20/80) copolymer is dominated by EA units, whereas the chain structure of the PY/EA (30/70) copolymer is dominated by PY units. Note that the PY/EA (30/70) copolymer is partly soluble in most of the solvents listed in Table 5, which is another evidence of the formation of the real copolymer. Additionally, there is a strong and broad absorption band from 4000 to 1700 cm^{-1} at the bottom of Fig. 3, which was regarded as the tail of an electronic absorption band in the near infrared field [27]. The broad band becomes stronger with an increase in PY content and finally PY/EA (90/10) copolymer exhibits almost the same IR spectrum as PPY [28,29], confirming that the PY unit predominates the copolymer structure.

IR spectra of doped and dedoped copolymers with PY feed content from 10 to 90 mol% are shown in Figs. 3–7. It is seen that IR spectra of the doped polymer substantially resemble those of dedoped polymer except for a small and relatively apparent absorption at 1650 cm^{-1}, suggesting that the dedoping process does not influence clearly the bond structure and polymerization degree of the PY/EA copolymers. However, the bands of virgin doped polymers from 4000 to 1700 cm^{-1}, as the characteristic band of electroconductive polymer, are stronger than those of dedoped polymers, implying that the dedoping process weakens the π-conjugated bond system.

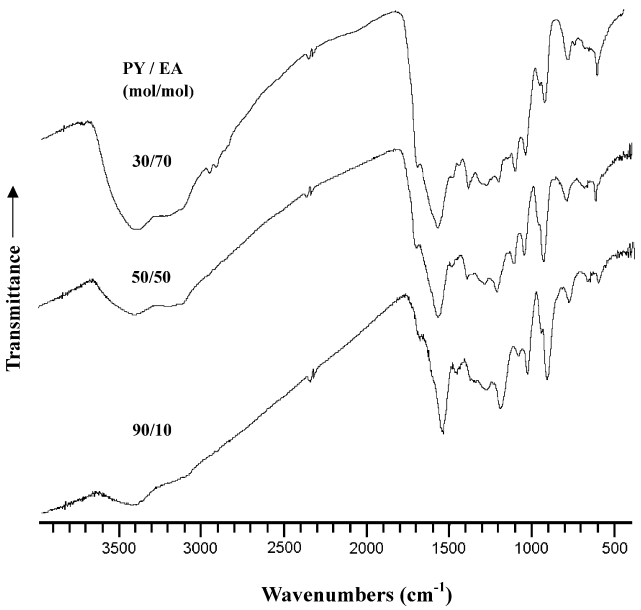

Fig. 4. IR spectra of the copolymer salts (doped form) with PY/EA molar ratios at 30/70. 50/50, and 90/10.

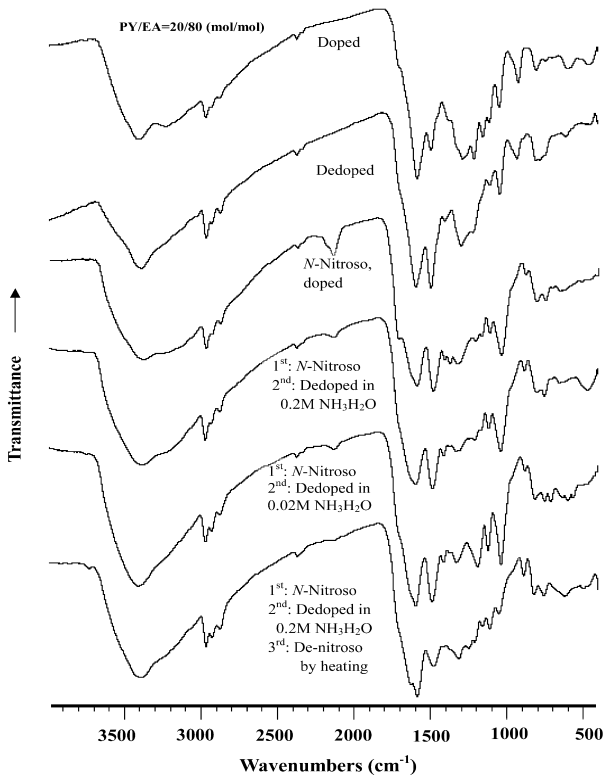

Fig. 5. IR spectra of PY/EA (20/80) copolymers at various states of (a) doped; (b) dedoped; (c) *N*-nitroso dedoped in 0.2 M $NH_3{\cdot}H_2O$; (d) *N*-nitroso dedoped in 0.02 M $NH_3{\cdot}H_2O$; (e) *N*-nitroso; doped form; (f) de-nitroso by heating.

IR spectra of PY/EA (20/80 and 10/90) copolymers at various states are shown in Figs. 5 and 6. After the *N*-nitrosation process, a new absorption at 2140 cm^{-1} appears clearly and the absorption at 1050 cm^{-1} becomes stronger, due to the presence of *N*-nitroso groups [30], implying an incorporation of *N*-nitroso groups into the copolymer chains. The absorptions at 2140 and 1050 cm^{-1} become obviously weak after dedoping process in $NH_3{\cdot}H_2O$. These phenomena reflect that *N*-nitroso groups are not stable and easy to disengage from polymer chain during dedoping process.

IR spectra of the de-nitroso copolymers with different PY/EA ratios are shown in Fig. 7. After the de-nitrosation reaction, the absorption at 2140 cm^{-1} becomes much weaker and the absorption at 1050 cm^{-1} becomes weaker. That is to say, just a simple heat treatment around 70 °C can

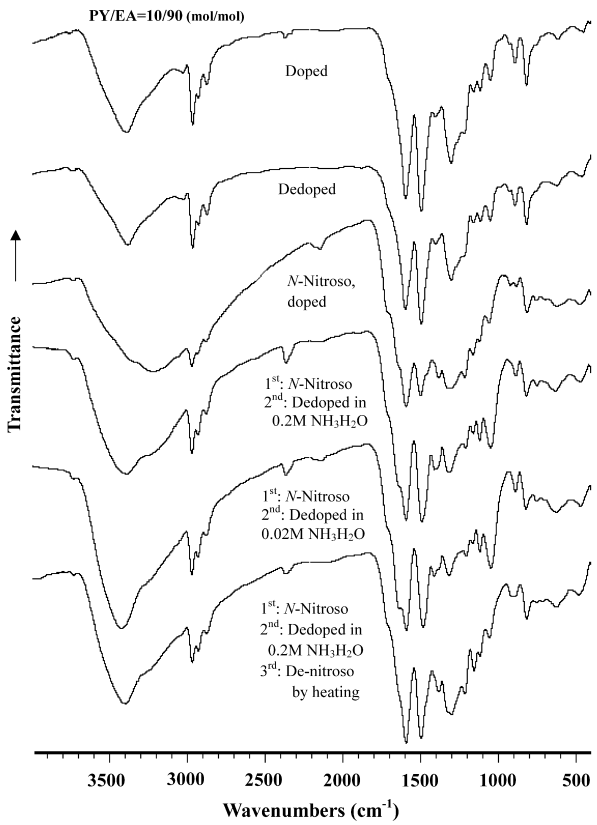

Fig. 6. IR spectra of PY/EA (10/90) copolymers with: (a) doped, (b) dedoped, (c) nitroso dedoped in 0.2 M $NH_3{\cdot}H_2O$, (d) nitroso dedoped in 0.02 M $NH_3{\cdot}H_2O$, (e) nitroso, doped form and (f) de-nitroso by heating.

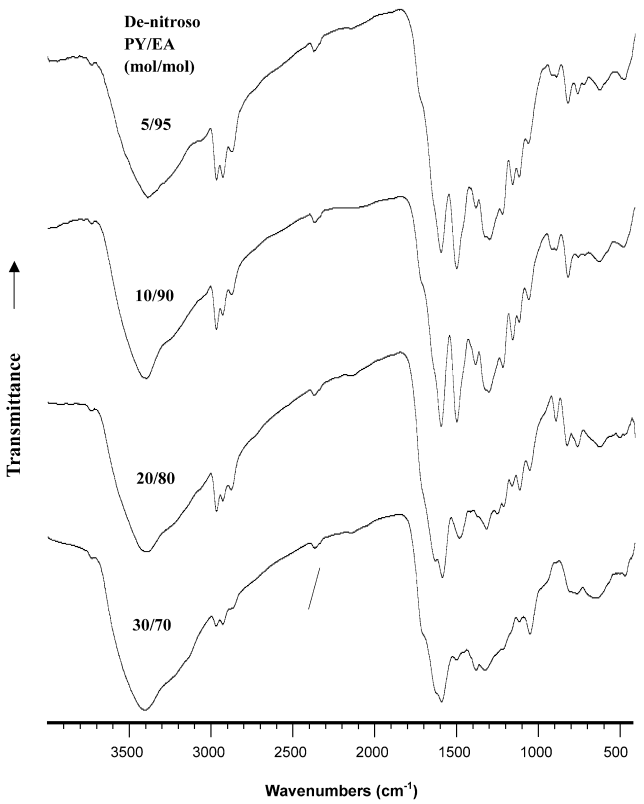

Fig. 7. IR spectra of de-nitroso PY/EA copolymers with different molar ratios.

remove the *N*-nitroso group after the formation process, indicating a regeneration of the polymers. This is an exhilarating phenomenon to improve the solution processability first by *N*-nitrosation (as discussed in Section 3.6) and finally regenerate the original macromolecular structure and thus the properties by a simple de-nitrosation. This is not possible for the other modifying methods, such as an incorporation of ring- or *N*-substituted alkyl or alkoxyl groups.

3.5. UV–vis spectra

Fig. 8 exhibits UV–vis absorption spectra of the copolymers in formic acid. Their first absorption appears at 359, 358, and 354 nm for the copolymers with PY feed content of 0, 5, and 10 mol%, respectively. The second absorption locates at 828, 837, and 824 nm for the copolymers with PY feed content of 0, 5, and 10 mol%, respectively. The first and second bands at 354–359 and 824–837 nm should correspond to $\pi \rightarrow \pi^*$ transition and $n \rightarrow \pi^*$ transition in the neutral form, respectively, [15,31,32]. It is found that with increasing PY content from 0 to 10 mol%, the wavelength of the both bands shifts to lower value as a whole and the relative intensity gets stronger continuously. Note that the PY/EA (5/95) copolymer exhibits a strong and broad band at much longer wavelength of 1100 nm. These results suggest that the conjugation length of the copolymers increases with the increase of PY content. Furthermore, pure PPY is not soluble in formic acid (see Table 5). Therefore the oxidative polymer from PY with EA is confirmed to be a copolymer of two monomers rather than a mixture of two homopolymers.

Fig. 8 shows UV–vis spectra of dedoped PY/EA (10/90) copolymer and its *N*-nitroso product. PY/EA (10/90)

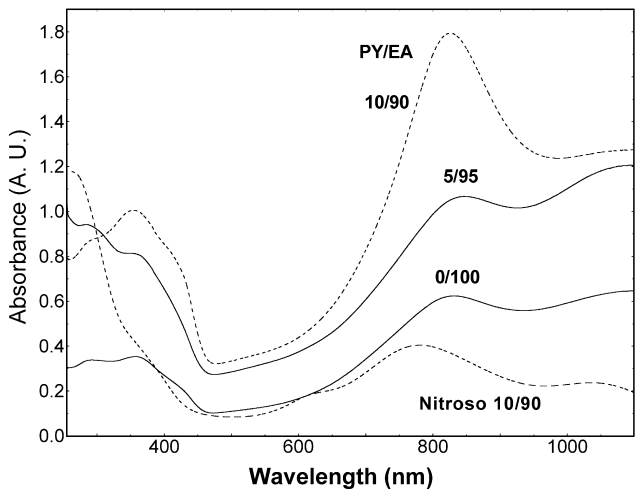

Fig. 8. UV-visible spectra of dedoped copolymers with the different PY/EA ratios and one *N*-nitroso dedoped copolymer at the concentration of 0.1 mg/6 ml formic acid.

copolymer exhibits the first band at 354 nm due to $\pi \rightarrow \pi^*$ transition [33], whereas the *N*-nitroso product shows a blue shift to 282 nm. The energy gap is related to the extent of conjugation between the adjacent rings in the polymer chain because this absorption shifts somewhat with increasing chain length. The hypsochromic shift results from the incorporation of electron-attraction *N*-nitroso group with a steric repulsion, leading to a decreased conjugation but an increased bandgap.

Other absorptions in a range of long wavelength are ascribed to the $n \rightarrow \pi^*$ transition (the exciton transition) [31,32]. There are also hypsochromic shifts from 827 to 781 nm due to *N*-nitrosation, and a new weak band at 620 nm appears. Possible reason is that the exciton transition is sensitive to a chain conformation related process because the *N*-nitroso group increases the chain rigidity and then restricts the conformation change. The relative intensity of the second band of the *N*-nitroso copolymer also gets much weaker, which suggests that the *N*-nitrosation weakens the π-conjugating system. A similar blue shift from 640 to 581 nm was observed due to the *N*-nitrosation of polyaniline [34]. It is found that the PY/EA (10/90) copolymer exhibiting UV–vis band at longer wavelength possesses longer conjugated bond than polyaniline, implying that the PY/EA (10/90) copolymer may exhibit higher electroconductivity.

The electronic absorption spectra of the dedoped PY/EA (5/95) copolymer and its dedoped *N*-nitroso compound in two $NH_3{\cdot}H_2O$ concentrations are shown in Fig. 9. It can be seen that the first band shows a clear blue shift owing to *N*-nitrosation. A clear hypsochromic shift of the second band from 850 to 795 nm can be also observed by contrast with un-nitroso copolymer. The blue-shift tendency agrees well with the above explanation about the UV–vis spectra of the dedoped PY/EA (10/90) copolymer and its dedoped *N*-nitroso compound. Note that the PY/EA (5/95) copolymer exhibits larger blue shift owing to the *N*-nitrosation than PY/EA (10/90) copolymer.

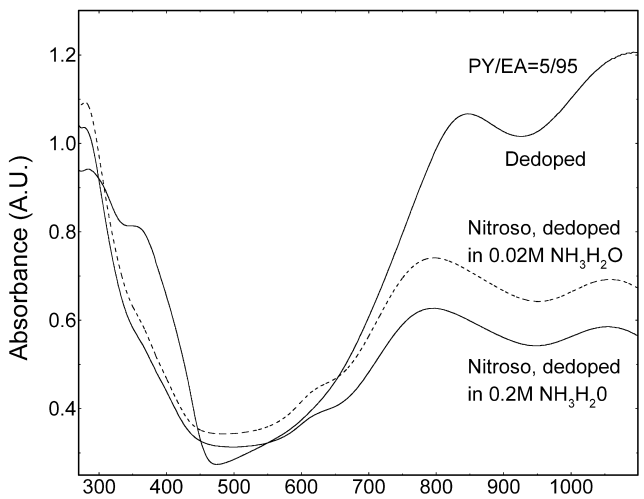

Fig. 9. UV–visible spectra of (a) the dedoped PY/EA (5/95) copolymer, (b) the nitroso copolymer dedoped in 0.02 M $NH_3{\cdot}H_2O$, and (c) the nitroso copolymer dedoped in 0.2 M $NH_3{\cdot}H_2O$ in HCOOH at the concentration of 0.1 mg/6 ml.

It appears that the hypsochromic shift also takes place and the relative intensity gets weaker with increasing $NH_3{\cdot}H_2O$ concentration for dedoping process. This seems contrast to the discussion of IR spectra, in which high alkalinity should be advantageous to the exclusion of the *N*-nitroso group, then leading to increases of the conjugation extent. Therefore, it could be concluded that the dedoping process of the *N*-nitroso copolymer in higher alkalinity can remove more dopant and then decrease the conjugation length. Furthermore, the exclusion of the dopant in two alkalinities from 0.02 to 0.2 M has greater influence on the conjugation extent than the elimination of *N*-nitroso groups from the copolymer chains.

3.6. Solubility

Poor processability is a serious problem for most of the π-conjugated polymers. The highly aromatic conducting polymers generally exhibit higher melting temperature than decomposition temperature, leading to a great difficulty of melt-processing route. Therefore, the improvement of the processability of the conducting polymers, especially PPY, should depend on the enhancement of the polymer solubility by chemical modification, because the solubility is one of the most important performances deciding the feasibility of solution-processing method. The semi-quantitative solubility of PY/EA copolymers in various solvents with wide characteristic parameters is summarized in Table 5. In contrast to a complete insolubility of PPY, the copolymers exhibit good solubility in the solvents with high boiling point, including NMP, *m*-cresol, DMF, formic acid, H_2SO_4, and DMSO. These solvents have solubility parameter, 23–27, dielectric constant > 12 and polarity index, 6.4–7.4. It seems that formic acid with the solubility parameter 25, dielectric constant 58 and polarity index 6.5 is an excellent solvent for the copolymer. The lower PY content, the better the solubility of the PY/EA copolymer in these solvents is. The increase of the solubility could be attributed to an incorporation of the ethyl groups [20] because the ethyl groups with a steric hindrance can lower the interchain action [19], increase the interchain distance and finally strengthen the interaction and affinity between polymer chains and solvent molecules.

The solubility of the PY/EA copolymers in the low-boiling-point solvents, such as $CHCl_3$, THF and CH_2Cl_2, is very interesting. The solubility of the dedoped copolymers with PY content from 10 to 20 mol% seems the best, implying the occurrence of the copolymerization effect expected. However, all of the copolymer HCl salts is completely insoluble in the solvents. Both doped and dedoped forms of the copolymers are completely insoluble in the solvents when the PY content exceeds 50 mol%. These phenomena should be ascribed to a steady increase in

Table 6
The solubility of *N*-nitroso PY/EA copolymers

Solvents	Solubility parameter ($J^{1/2}/cm^{3/2}$)	Dielectric constant	Polarity index	Solubility of *N*-nitroso PY/EA copolymers and solution color[a]						
				5/95	10/90		20/80		30/70	
				De-0.02/-0.2[b]	Doped	De-0.02/-0.2[b]	Doped	De-0.02/-0.2[b]	Doped	De-0.02/-0.2[b]
NMP	23	32	6.7	S(V)	S(UL)	S/MS(MO)	S(Ma)	S/MS(Ma)	PS(Ma)	PS(Ma)
DMSO	27	47	7.2	S(SC)	PS(MO)	PS(LR)	PS(M)	PS(M)	PS(RO)	PS(RO)
DMF	25	38	6.4	S(SC)	PS(MO)	PS/MS(V)	PS(M)	PS(M)	PS(Ma)	PS(Ma)
Formic acid	25	58	6.5	S(BO)	S(BO)	S(BO)	MS(BO)	MS(BO)	PS(Bl)	MS(Gr)
m-Cresol	23	12	7.4	S(BO)	MS(G)	S/MS(G)	S(BO)	S/MS(MO)	PS(Bl)	MS(Gr)
H_2SO_4	–	101	–	S(V)	PS(DM)	PS(V)	PS(V)	PS(V)	MS(M)	MS(M)
$CHCl_3$	19	5	4.1	MS(M)	PS(Ma)	S(Ma)	MS(YM)	PS/MS(LM)	PS(RM)	MS(Ma)
THF	20	7	4.0	S(SC)	PS(Ma)	S(Ma)	PS(SC)	MS(LM)	PS(M)	MS(V)
CH_2Cl_2	20	9	–	PS(SC)	SS(LG)	PS/S(Ma)	S(YM)	S/MS(M)	PS(M)	MS(V)

[a] The letters in the parentheses mean solution color.
[b] De-0.02, dedoped form with 0.02 M $NH_3{\cdot}H_2O$; De-0.2, dedoped form with 0.2 M $NH_3{\cdot}H_2O$.

conjugating extent and stiffness of the chains by the incorporation of the dopant or the increase of PY content.

The solubility of four *N*-nitroso copolymers with PY feed content from 5 to 30 mol% is described in Table 6. In contrast to the PY/EA copolymers, the *N*-nitroso copolymers exhibit an enhanced solubility in the solvents with high boiling point and large solubility parameter, dielectric constant and polarity index, i.e. NMP, *m*-cresol, DMF, formic acid, together with the change of solution color which reflects the change of conjugated structure. The increased solubility can be attributed to a decreased regularity of the polymer chains and an increased affinity (interaction) to solvents by an incorporation of polar nitroso groups. However, the increase of solubility in low polar solvents is not apparent. All of the copolymer salts, bases and their *N*-nitroso products are totally insoluble in simple aromatics such as benzene and toluene (not shown in Tables 5 and 6). Anyhow, it is concluded that the insolubility of the PPY has been overcome greatly by a copolymerization of PY with EA monomers. Therefore its solution processability is also enhanced significantly, as discussed below.

3.7. Film formability

Four solvents including NMP, DMSO, formic acid and THF were selected for the preparation of the copolymer films. Although the film formability of the copolymers in DMSO and formic acid is not good enough because of the poor solubility in DMSO and bad gelation ability in formic acid during the evaporation of formic acid, the film formability in NMP and THF is very good, as listed in Table 7. In particular, the PY/EA (5/95) copolymers in three forms exhibit excellent film formability. After the solvent evaporated, most of thin and uniform PY/EA copolymer films on glass were easily peeled off upon immersion in water, indicating good film flexibility. Note that the film formability of the copolymers with PY content ≥ 30 mol% cannot be determined because of their poor solubility.

Thickness of the PY/EA copolymer films formed depends significantly on the volatility of the solvents. When NMP with low volatility was used, the film thickness ranges from 40 to 80 μm, whereas the film thickness increases to 110–160 μm with highly volatile THF. The average thickness of the copolymer films is close to 100 μm of the PPY film prepared by electro-deposition on a rotating electrode [35]. It is seen from Table 7 that with the increase of EA content, the films of the PY/EA copolymers become more lustrous, smoother and tougher. *N*-nitrosation of PY/EA copolymers increases their solubility and further improves film formability. At the same time the luster and the smoothness of *N*-nitroso copolymer films formed seem to be improved slightly. Therefore, the solution processability of the PPY has been remarkably improved by a combination of a copolymerization of PY and EA monomers with a subsequent *N*-nitrosation.

Table 7
The film formability of PY/EA copolymers in NMP and THF at the same copolymer concentration of 5 g/100 ml solvent

PY/EA molar ratio	Copolymer form	Solvent	Film thickness (μm)	Film appearance	Film-forming ability	Film-peeled ability
0/100	Doped	NMP	40	Dark, metallic luster, relatively smooth	Good	Good
	Dedoped	NMP	10	Dark, strong metallic luster, smooth	Good	Fair
5/95	Dedoped	NMP	20	Dark, strong metallic luster, smooth	Excellent	Good
	N-De-0.2[a]	NMP	20(30)	Dark, strong metallic luster, smooth	Excellent	Good
	(N-De-0.02)[a]	THF	110(160)	Dark, strong metallic luster, smooth	Excellent	Excellent
10/90	Doped	NMP	50	Dark, metallic luster, relatively smooth	Fair	Good
	Dedoped	NMP	10	Dark, strong metallic luster, smooth	Good	Good
	N-nitroso doped	NMP	10	Dark, metallic luster, relatively smooth	Fair	Good
	N-De-0.2[a]	NMP	50(20)	Dark, metallic luster, relatively smooth	Good	Good
	(N-De-0.02)[a]	THF	150(140)	Dark, strong metallic luster, smooth	Good	Excellent
20/80	Doped	NMP	80	Dark, shimmer, relatively smooth	Fair	Fair
	Dedoped	NMP	10	Dark, metallic luster, relatively smooth	Good	Good
		THF	150	Dark, strong metallic luster, smooth	Good	Excellent
	N-nitroso doped	NMP	10	Dark, metallic luster, smooth	Good	Good
	N-De-0.2[a]	THF	50	Dark red, strong metallic luster, smooth	Good	Excellent
	(N-De-0.02)[a]	NMP	10(20)	Dark, metallic luster, smooth	Good	Good

[a] N-De-0.02, *N*-nitroso dedoped form with 0.02 M $NH_3 \cdot H_2O$; N-De-0.2, *N*-nitroso dedoped form with 0.2 M $NH_3 \cdot H_2O$.

3.8. Electroconductivity

The electrical conductivity of the PY/EA polymers appears to be directly related to the PY/EA ratio, as shown in Fig. 2. It is found that the conductivity of the original doped copolymers decreases with the increase in mole fraction of the second monomer unit in the copolymers. In particular, the copolymers exhibit the lowest conductivity at the PY/EA molar ratio of 30/70. It is interesting that the conductivity and polymerization yield show very similar dependency on the PY/EA ratio. The reduction in the conductivity of the copolymers should be associated with a less efficient charge transport that could easily arise from the interruption of the order of polaron lattice because of the variation of π-conjugation and resonance effect with the formation of the PY–EA linkages when a second monomer unit or segment of different electronic structure is incorporated. Similar decline of conductivity has also been reported for PY–aniline or PY–thiophene copolymers [36]. The maximum loss in conductivity appeared around PY content of 30 mol% further confirms the presence of randomly distributed PY and EA units or segments in the copolymers. However, as shown in Fig. 2, the conductivity will decrease greatly with the *N*-nitrosation of doped PY/EA polymers because the incorporation of *N*-nitroso groups into the polymers destroys their large π-conjugation structure in the macromolecular chain direction to some extent although all of the *N*-nitroso doped PY/EA polymers is still bluish black [34], an indication of π-conjugated structure.

3.9. Thermal stability

TG and DTG curves of the copolymers with seven PY/EA ratios in air are shown in Fig. 10. The polymers exhibit a 3–7% weight-loss process at 40 to 100 °C due to water evaporation and a major decomposition starting at around 250 °C. It is surprising that at the PY content of

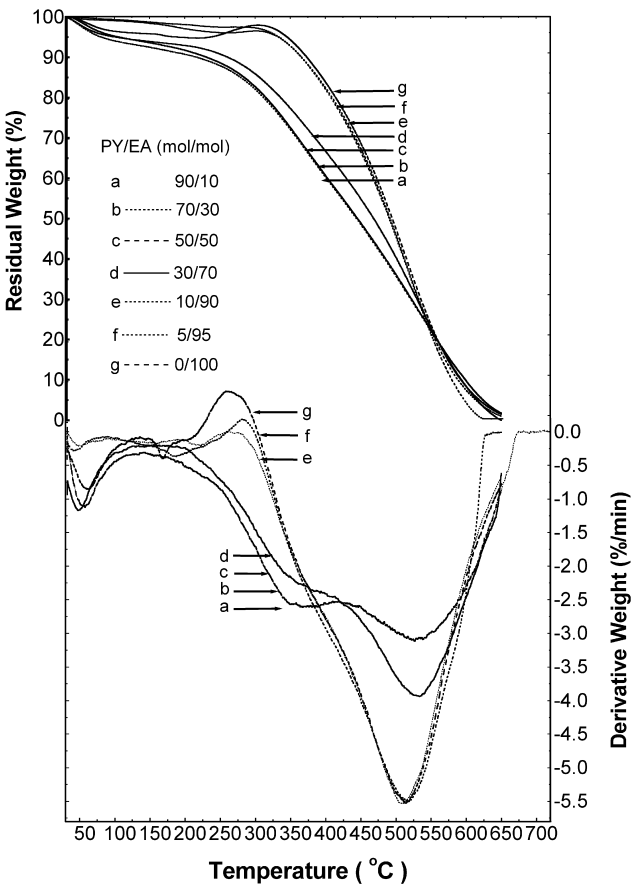

Fig. 10. TG and TGA curves of the copolymers with different PY/EA molar ratios in air flow.

Table 8
Thermally stable parameters of PY/EA copolymers with an oxidant $[(NH_4)_2S_2O_8]$/monomer molar ratio of 1/2 in 1 M HCl at a polymerization time of 8 h in air flow

PY/EA molar ratio	T_d(°C)	T_{dm}(°C)	$(d\alpha/dt)_m$(%/min)	Char yield at 500 °C (wt%)	E (kJ/mol)	n	Ln Z (min^{-1})
0/100	387	515	5.50	48.0	13	4.7	1.0
5/95	373	518	5.48	44.9	9.4	3.9	0.50
10/90	368	512	5.50	46.7	13	4.8	1.2
30/70	303	532	3.91	40.5	9.5	3.6	0.68
50/50	288	365, 530	2.59, 3.06	36.3	4.4	2.1	0.32
70/30	284	369, 524	2.91, 2.91	35.9	4.6	2.2	0.35
90/10	280	369, 515	2.72, 2.76	33.9	2.3	1.6	1.0

0–10 mol%, the residual weight of the copolymers at 250–320 °C increases abnormally, perhaps due to the formation of carboxyl group by an oxidation of the ethyl group in the EA units [37]. It is the oxidative stabilization that weakens the decomposition peak around 360 °C, because the copolymers with the PY content of 30–90 mol% exhibit an explicit decomposition peak at 365–369 °C. However, all the copolymers exhibit a clear decomposition peak at 512–530 °C, and corresponding weight-loss rate is proportional to EA unit content. Table 8 lists the thermal degradation parameters of the copolymers. With increasing EA content, the temperature (T_d), char yield at 500 °C, activation energy (E), and order (n) of the decomposition [38,39] all increase substantially because of the oxidative stabilization from EA units [37], while an increase in the maximum decomposition rate $[(d\alpha/dt)_m]$ at an elevated temperature with increasing EA content should be ascribed to a steadily increased oxygen content within the polymers from the oxidative stabilization. This illuminates a fact that the presence of the ethyl groups will not lower the thermostability because the elimination of the ethyl groups will be prevented to some extent by the oxidative stabilization. Note that the PY/EA (30/70) copolymer with the highest MW exhibits the highest temperature at the maximum weight-loss rate (T_{dm}) [37], confirming the occurrence of the copolymerization once again.

4. Conclusions

The PY/EA copolymer particles have been successfully and directly synthesized by a heterohomogeneous oxidative polymerization. The size and its distribution of the particles formed in situ during the polymerization decrease with prolongating the polymerization time or doping or *N*-nitrosating. There is an obvious dependency of polymerization yield and rate, MW, solubility, film-forming ability, electroconductivity, and thermostability of the copolymers on PY/EA comonomer ratio. The minimum polymerization yield and MW are observed at the PY/EA molar ratio of 30/70 and 5/95, respectively, suggesting lower reactivity of copolymerization between PY and EA than that of both homopolymerizations. The PY/EA copolymers have better solubility in the solvents with solubility parameter from 23 to 27, dielectric constant >12 and polarity index from 6.4 to 7.4, such as formic acid. The solution film formability of the copolymers with PY content <30 mol% becomes better and the films formed get more lustrous, smoother and tougher with increasing EA content. The solubility and film formability could be further improved by *N*-nitrosation on the copolymers. Though the incorporation of the *N*-nitroso groups shortens the conjugated length, the *N*-nitroso groups can be easily removed from the chains by a simple heating, leading to a recovery of the initial conjugated system. The insolubility of PPY can be overcome to some extent by copolymerizing with EA and then *N*-nitrosating the copolymers. The copolymers usually show much lower electroconductivity than the respective homopolymers due to the interruption of the polaron lattice with incorporating the second monomer unit. The thermostability of the PY/EA copolymers increases with increasing EA content due to an oxidative stabilization from ethyl group.

Acknowledgements

This project is supported by (1) The two National Natural Science Funds of China (20174028 and 20274030); (2) the Foundation of Shanghai Leading Academic Discipline, Donghua University, China; (3) The Fund of Shanghai Nano Science Technology, China (0259nm022); (4) Shanghai Key Laboratory of Molecular Catalysis and Innovative Materials, Fudan University, China. The authors would like to thank Prof. Dr Dong-Yuan Zhao (Fudan University) and Hong-Tao Shao (Tongji University) for their valuable helps.

References

[1] Li XG, Huang MR, Duan W, Yang YL. Chem Rev 2002;102:2925.
[2] Morita M. Makromol Chem 1993;194:2361.
[3] Heinze J. Synth Met 1991;41–43:2805.
[4] Ochmanska J, Pichup PG. J Electroanal Chem 1991;297:197.
[5] Iyoda T, Ohtani A, Honda K, Shimidzu T. Macromolecules 1990;23:1971.
[6] Campbell TE, Hodgson AJ, Wallace GG. Electroanalysis 1999;11:215.

[7] Riul Jr A, Gallardo SAM, Mello SV. Synth Met 2003;132:109.
[8] Camalet JL, Lacroix JC, Aeiyach S. Synth Met 1998;93:133.
[9] Lacroix JC, Camalet JL, Aeiyach S. J Electroanal Chem 2000;481:76.
[10] Salamone JC. Encyclopedia of polymeric materials. Boca Raton, FL: CRC Press; 1996.
[11] Nalwa HS, Handbook of organic conductive molecules and polymers, vol. 1–4. Chichester: Wiley; 1997.
[12] Tourillon G. In: Skotheim TA, editor. Handbook of conducting polymers. New York: Marcel Dekker; 1986. p. 294.
[13] Schemid AL, Lira LM, Co'rdoba de Torresi SI. Electrochim Acta 2002;47:2005.
[14] Machida S, Miyata S. Polym Prepr Jpn 1987;36:1886.
[15] Leclerc M, Guay J, Dao LH. Macromolecules 1989;22:649.
[16] Reynolds JR, Poropatic PA, Toyooka RL. Macromolecules 1987;20: 958.
[17] Asavapiriyanont S, Chandler GK, Gunawardena GA. J Electroanal Chem 1984;177:299.
[18] Leclerc M, Fuay J, Dao LH. Macromolecules 1989;22:649.
[19] Wu QJ, Xue ZJ, Qi ZN. Synth Met 2000;108:107.
[20] Kim JW, Jang WH, Choi HJ. Synth Met 2001;119:173.
21 Li XG, Chen RF, Huang MR, Zhu MF, Chen Q. J Polym Sci Part A Polym Chem 2003;41. in press.
[22] Sak-Bosbar M, Budimir MV, Kovac S. J Polym Sci Part A Polym Chem 1992;30:1609.
[23] Kang ET, Neoh KG, Tan TC. J Macromol Sci Chem 1987;A24:631.
[24] Masuda H, Tanaka S, Kaeriyama K. J Polym Sci Polym Chem Ed 1990;28:1031.
[25] Jin JY, Teramae N, Haraguchi H. Bunseki Kagaku 1991;40:799.
[26] Li XG, Wang LX, Huang MR, Lu YQ, Zhu MF, Menner A, Springer J. Polymer 2001;42:6095.
[27] Tang J, Jing X, Wang F. Synth Met 1988;24:231.
[28] Chao TH, March J. J Polym Sci Part A Polym Chem 1988;26:743.
[29] Neoh KG, Tan TC, Kang ET. Polymer 1988;29:553.
[30] Bicak N, Senkal BF. React Funct Polym 1998;36:71.
[31] Pandey SS, Annapoomi S, Malhtra BD. Macromolecules 1993;26: 3190.
[32] Peters EM, Van Dyke JD. J Polym Sci Part A Polym Chem 1992;30: 1891.
[33] Kurachi K, Kise H. Polym J 1994;26:1325.
[34] Sharma AL, Ammapoorni S, Malhotra BD. Polymer 2001;42:8307.
[35] Choi J, Chipara M, Xu B, Yang CS, Doudin B, Dowben PA. Chem Phys Lett 2001;343:193.
[36] Lim VWL, Kang ET, Neoh KG, Ma ZH, Tan KL. Appl Surf Sci 2001; 181:317.
[37] Wang XH, Geng YH, Wang LX, Jing XB, Wang FS. Synth Met 1995; 69:263.
[38] Huang MR, Li XG. J Appl Polym Sci 1998;68:293.
[39] Huang MR, Li XG, Yang YL. Polym Degrad Stab 2001;71:31.